CMS Physics Analysis Summary

Contact: cms-pag-conveners-exotica@cern.ch 2011/07/22

Search for Heavy Stable Charged Particles in pp collisions at $\sqrt{s} = 7$ TeV

The CMS Collaboration

Abstract

The result of a search at the LHC for heavy stable charged particles produced in pp collisions at $\sqrt{s} = 7$ TeV is described. The data sample was collected with the CMS detector and corresponds to an integrated luminosity of 1.09 fb^{-1}. Momentum and ionization-energy-loss measurements in the inner tracker detector are used to identify tracks compatible with heavy slow-moving particles. Additionally, tracks passing muon identification criteria are required to have a large time-of-flight consistent with a slow moving particle. In both cases, the final data samples are consistent with the expected background estimated by a data driven technique. This result is interpreted within the context of models with a (quasi-)stable gluino, scalar top-quark models, and scalar tau. Lower limits at 95% C.L. on the mass of stable gluinos (scalar top-quarks) are set at 899 (620) GeV/c^2. The lower mass limit for a scalar tau is set at 293 GeV/c^2. A limit of 808 (515) GeV/c^2 is also set for a stable gluino (scalar top-quark) that becomes neutral before reaching the muon detectors.

1 Introduction

Heavy Stable (or long-lived) Charged Particles (HSCPs) appear in various extensions to the Standard Model (SM) [1]. An example of an HSCP with early discovery potential at the LHC was presented in Ref. [2]. If the lifetime of an HSCP produced at the Large Hadron Collider (LHC) is longer than a few nanoseconds, the particle will travel over distances that are comparable or larger than the size of a typical particle detector. In addition, if the HSCP mass is $\gtrsim$100 GeV/c^2, a significant fraction of these particles will have a velocity, $\beta \equiv v/c$, smaller than 0.9. These HSCPs will be directly observable through the distinctive signature of a high momentum (p) particle with an anomalously large rate of energy loss through ionization (dE/dx) and an anomalously long time-of-flight (TOF).

Previous collider searches for HSCPs have often been performed under the assumption that these particles lose energy primarily through low-momentum-transfer interactions, even if they are strongly interacting, and are therefore likely to reach the outer muon systems of the detectors and be identified as muons [1, 3–9].

The interactions with matter experienced by a strongly-interacting HSCP, which is expected to form a bound state (R-hadron) [10] in the process of hadronization, can lead to it flipping the sign of its electric charge or becoming neutral. A recent study [11] on the modeling of nuclear interactions of HSCPs traveling through matter, favors a scenario of charge suppression. In this model, the majority of R-hadrons containing a gluino, $\widetilde{\mathrm{g}}$ (the supersymmetric partner of the gluon), or a supersymmetric bottom squark, are expected to emerge as neutral particles after traversing an amount of material typical of the detectors operating at LEP, the Tevatron, or LHC. If this model is correct, the majority of these HSCPs would not be observed in the muon system of a typical collider detector. Experimental strategies that do not rely on the muon-like behavior for the HSCPs are therefore of great importance. For instance, searches have been performed for very slow ($\beta \lesssim 0.4$) R-hadrons containing a gluino brought to rest in the detector [12, 13]. Other searches [4, 5] have exploited only inner tracker and calorimeter information.

In this article we present a search for HSCPs produced in pp collisions at $\sqrt{s} = 7$ TeV at the LHC with the Compact Muon Solenoid (CMS) detector [14]. The search is based on the data sample collected in 2011 corresponding to an integrated luminosity of 1.09 fb^{-1}. Data were collected with either high transverse momentum (p_{T}) muon or missing transverse energy ($E_{\mathrm{T}}^{\mathrm{miss}}$) triggers. The analysis isolates HSCP candidates by selecting tracks reconstructed in the inner tracker detector with large dE/dx and high p_{T}. A second selection additionally requires that the tracks be muon identified and have a large TOF. For both selections, the candidate's mass is then calculated from the measured p and dE/dx. This analysis improves on our previously published result [5] through: increased luminosity, first use of muon time-of-flight information, final selection optimization for best expected limits, and new isolation requirements.

2 Signal Simulation

A number of simulated signal samples are used in this analysis. As in [5], events with pair production of $\widetilde{\mathrm{g}}$ and supersymmetric top squark ($\tilde{\mathrm{t}}_1$), with mass values in the range 130-1100 GeV/c^2, are generated with PYTHIA v6.422 [15]. For gluino production, we set the squark masses very high (>7 TeV) so that the cross section is dominated by gluino pair production. In order to study the uncertainties related to the underlying production processes, samples are produced with three different multi-parton interaction (MPI) models: DW with CTEQ5L PDF (used in [4]), D6T with CTEQ6L1 PDF (used in [5]) and Z2 with CTEQ6L1 PDF. The latter

model features larger initial state radiation. The full study is performed with samples using D6T.

The fraction, f, of produced $\widetilde{\mathrm{g}}$ hadronizing into a $\widetilde{\mathrm{g}}$-gluon state (R-gluonball) is an unknown parameter of the hadronization model and affects the fraction of R-hadrons that are neutral at production. As in [5], results are obtained for two different values of f, 0.1 and 0.5. Unless specified otherwise, the value $f = 0.1$ should be assumed. As for [5], two scenarios of R-hadron strong interactions with matter are considered: the first follows the model defined in [16, 17], while the second is one of complete charge suppression, where each nuclear interaction suffered by the R-hadron causes it to become neutral. The tracker-only selection, defined below, is expected to have sensitivity even in the second scenario.

In this analysis, the minimal gauge mediated supersymmetry breaking (mGMSB) model [18] is selected as a benchmark for lepton-like HSCPs. Production of supersymmetric quasi-stable leptons ($\tilde{\tau}_1$) at the LHC can proceed either directly or via production of heavier supersymmetric particles (mainly squarks and gluino pairs), which decay leading to one or more $\tilde{\tau}_1$ particles at the end of the decay chain. The latter process is in general larger due to the strong nature of the production process. Two benchmark points on the SPS line 7 [19] are considered. The particle mass spectrum and the decay table are produced with the program ISASUGRA [20] version 7.69. The parameter values corresponding to the two considered points are as follows:

- $\tilde{\tau}(156)$: $N = 3$, $\Lambda = 50000$ GeV, $M = 100000$ GeV, $\tan\beta = 10$, $sign(\mu) = 1$, $c_{grav} = 10000$
- $\tilde{\tau}(247)$: $N = 3$, $\Lambda = 80000$ GeV, $M = 160000$ GeV, $\tan\beta = 10$, $sign(\mu) = 1$, $c_{grav} = 10000$

The corresponding $\tilde{\tau}_1$ masses are 155.8 and 247 GeV/c^2. The squark and gluino masses are of about 1.1 and 1.7 TeV/c^2, respectively. A few more mass points are obtained by varying the Λ parameter in order to cover a mass range from 100 to 500 GeV/c^2. For all points, the squark and gluino production cross sections are between one and two orders of magnitude higher than that of direct $\tilde{\tau}_1$ pair production.

In all Monte Carlo samples, the primary collision event is overlaid with minimum bias events to model the pile-up in data.

3 The CMS Detector

The central feature of the CMS apparatus is a superconducting solenoid of 6 m internal diameter. Within the field volume are the silicon pixel and strip tracker, the crystal electromagnetic calorimeter (ECAL) and the brass/scintillator hadron calorimeter (HCAL). Muons are measured in gas-ionization detectors embedded in the steel return yoke. In addition to the barrel and endcap detectors, CMS has extensive forward calorimetry. The muons are measured in the pseudorapidity range $|\eta| < 2.4$, with detection planes made using three technologies: Drift Tubes (DTs), Cathode Strip Chambers (CSCs), and Resistive Plate Chambers (RPCs). Matching the muons to the tracks measured in the silicon tracker results in a transverse momentum resolution between 1 and 5 %, for p_{T} values up to 1 TeV/c. The inner tracker measures charged particles within the pseudorapidity range $|\eta| < 2.5$. It consists of 1440 silicon pixel and 15 148 silicon strip detector modules and is located in the 3.8 T field of the superconducting solenoid. It provides an impact parameter resolution of $\sim$15 μm and a p_{T} resolution of about 1.5 % for 100 GeV/c particles. The CMS trigger system consists of a two layered system. The first level (L1) of the CMS trigger system, composed of custom hardware processors, uses information

from the calorimeters and muon detectors to select, the most interesting events. The High Level Trigger (HLT) processor farm further decreases the event rate from around 100 kHz to around 300 Hz, before data storage.

A detailed description of the CMS detector can be found elsewhere [14]. A major addition to this analysis with respect to that in [5] is the use of time-of-flight information from the muon system. This measurement is described in more detail in this section.

3.1 DT TOF Measurement

In each wheel of the barrel of CMS there are four muon stations. Each station (except the outermost) contains three super-layers (SL), each composed of four DT layers. Hits in the muon system are combined to form local track elements (two dimensional $r-\phi$ segments). Only SLs in the $r-\phi$ projections are used since their time resolution is a factor of 2 better than the θ view SL. Fits of these elements yield, among other things, an off-time correction (δ_t) which is necessary only for non-prompt muons or prompt HSCP candidates and is common to all hits of a 2D segment. The average value, $\langle\delta_t\rangle$, for muons originating at the primary vertex of the correct bunch crossing (BX) should be equal to zero in any chamber within the time measurement accuracy. For HSCP particles that travel with velocity $\beta < 1$, it is expected that $\langle\delta_t\rangle > 0$.

The β value is related to δ_t by:

$$\frac{1}{\beta} = 1 + \frac{c\delta_t}{L} \tag{1}$$

where L is the flight distance and c is the speed of light. For a given candidate in the barrel region, we calculate the average value of the inverse of β, $\langle\frac{1}{\beta}\rangle$, and its uncertainty, $\sigma_{\langle\beta^{-1}\rangle}$, using each hit $i = 1, n_j$ in each SL $j = 1, N_{SL}$, from the following relationships:

$$\left\langle\frac{1}{\beta}\right\rangle = \frac{\sum_{j=1}^{N_{SL}} \frac{n_j-2}{n_j} \sum_{i=1}^{n_j} \left(\frac{1}{\beta}\right)_{ij} L_{ij}^2}{\sum_{j=1}^{N_{SL}} \frac{n_j-2}{n_j} \sum_{i=1}^{n_j} L_{ij}^2} \tag{2}$$

$$\sigma_{\langle\beta^{-1}\rangle} = \sqrt{\frac{\sum_{j=1}^{N_{SL}} \frac{n_j-2}{n_j} \sum_{i=1}^{n_j} \left\{\left(\frac{1}{\beta}\right)_{ij} - \left\langle\frac{1}{\beta}\right\rangle\right\}^2 L_{ij}^2}{\sum_{j=1}^{N_{SL}} \frac{n_j-2}{n_j} \sum_{i=1}^{n_j} L_{ij}^2}} \tag{3}$$

Figure 1 shows the distribution of the β^{-1} measurement for the candidates passing the tracker-plus-muon selection (defined in Sec. 4) in the barrel region.

3.2 CSC TOF Measurement

The Cathode Strip Chambers (CSC) measure the position of charged particles using a nearly orthogonal layout of anode wires and cathode strips. Both anode wires and cathode strips are used by this analysis to measure the candidate timing. The timing from the CSC system has been calibrated such that the average time of all measurements from muons emerging from the nominal collision point would be zero on average. The muon β^{-1} measurement is calculated as the weighted average of the individual β^{-1} measurements along the track. The weight for each measurement is determined as the distance from the nominal collision point squared divided by the time measurement uncertainty. To reduce the impact of outliers in

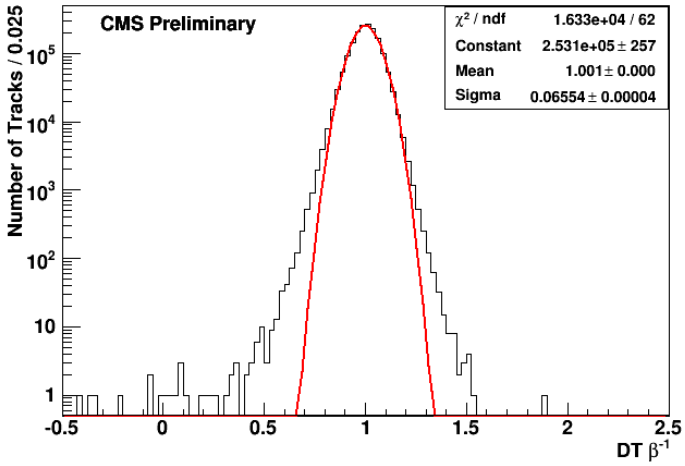

Figure 1: Distribution of β^{-1} for the candidates passing the tracker-plus-muon selection in the barrel region.

the anode wire measurement distribution, any CSC β^{-1} measurement which is more than 3 standard deviations away from the mean of the measurements is removed from the fit.

Figure 2 shows the distribution of the β^{-1} measurement for the candidates passing the tracker-plus-muon selection in the forward region.

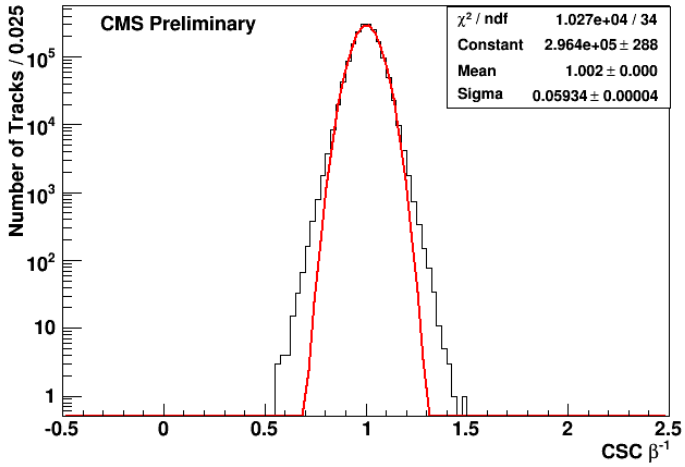

Figure 2: Distribution of β^{-1} for the candidates passing the tracker-plus-muon selection in the forward region.

4 Trigger and Data Selection

We use triggers requiring a high-transverse-momentum muon ($p_T > 30$ GeV/c) or missing transverse energy ($E_{\mathrm{T}}^{\mathrm{miss}} > 150$ GeV) computed out of jets reconstructed using the particle flow reconstruction [21], which provides a list of particles for each event. Jet clustering is performed with the anti-k_{T} algorithm [22] with a size parameter of 0.5. Triggering on $E_{\mathrm{T}}^{\mathrm{miss}}$ allows searching for HSCPs failing muon identification or emerging mainly as neutral particles after travers-

ing the calorimeters. At level-1 the muon trigger accepts tracks that produce signals in the RPC detectors either in the 25 ns wide time window centered around the collision bunch crossing or in the following 25 ns wide time window. This operation mode is particularly suited for detecting late tracks in the muon system and is only possible as long as collisions are separated by two or more LHC clock cycles. The DT and CSC triggers are also used for in-time bunch crossings.

The analysis makes use of two offline selections. In the first selection, referred to as "*tracker-only*", the HSCP candidates are searched for as individual tracks reconstructed in the inner tracker detector with large dE/dx and p_{T}. A second selection, referred to as "*tracker-plus-muon*", additionally requires that the track is identified as a muon from a global fit [23] of consistent measurements in the inner tracker and in the outer muon detectors, and has a large TOF. Events selected online with both the muon and $E_{\mathrm{T}}^{\mathrm{miss}}$ triggers are used in each of these two offline selections to maximize the sensitivity to HSCP signals.

As in [5], the adopted dE/dx estimators are I_h and I_{as}:

$$I_h = \left(\frac{1}{N}\sum_i c_i^k\right)^{1/k}, \tag{4}$$

where c_i is the charge per unit path length in the detector of the i-th measurement for a given track.

$$I_{as} = \frac{3}{N} \times \left(\frac{1}{12N} + \sum_{i=1}^{N}\left[P_i \times \left(P_i - \frac{2i-1}{2N}\right)^2\right]\right), \tag{5}$$

where N is the number of charge measurements in the silicon-strip detectors, P_i is the probability for a minimum–ionizing particle (MIP) to produce a charge smaller or equal to the i–th charge measurement for the observed path length in the detector, and the sum is over the track measurements ordered in terms of increasing P_i. The I_h estimator is computed using both silicon strip and pixel measurements. The I_{as} estimator is instead computed using only silicon strip measurements.

For both offline selections, candidates are pre-selected by requiring p_{T} measured by the inner tracker to be greater than 35 GeV/c, relative uncertainty on the p_T smaller than 0.25, track $\chi^2/d.o.f. < 5$, $|\eta| < 1.5$ and impact parameter $\sqrt{d_z^2 + d_{xy}^2} < 2$ cm where d_z and d_{xy} are the longitudinal and transverse impact parameters with respect to the reconstructed primary vertex. Candidates must also have at least two measurements in the silicon pixel detectors and at least eleven measurements in the inner tracking detectors. No more than 20% of the inner tracker layers must be missing between the first and last measurement of the track. A cleaning procedure is applied to the track measurements in the silicon strip detectors as described in [5]. Candidates are required to have at least four silicon strip measurements passing the cleaning criteria and, therefore, used for the dE/dx measurement. Candidate tracks are required to have $I_h > 3$ MeV/cm for the initial selection. For the tracker-plus-muon candidates, the additional requirements of $1/\beta > 1$, where β is measured from TOF, and $\sigma_{\beta^{-1}} < 0.07$, where $\sigma_{\beta^{-1}}$ is the uncertainty on $1/\beta$ are applied. The number of independent measurements used for the TOF computation must be greater than seven.

This analysis requires the track candidates to be loosely isolated as measured by both the inner tracker and the calorimeters. Inner tracker isolation is calculated by considering all tracks reconstructed in the inner tracking detector whose direction has a distance from the candidate track direction, $\Delta R \equiv \sqrt{(\Delta\varphi)^2 + (\Delta\eta)^2} < 0.3$. The scalar sum of the p_T of these tracks, with the

exception of the candidate track, is then required to be less than 50 (100) GeV/c for the tracker-only (tracker-plus-muon) selection. Calorimeter isolation is calculated as the ratio between the sum of the energies measured in each ECAL and HCAL tower, whose direction computed from the nominal center of the detector has a distance $\Delta R < 0.3$ from the candidate direction, and the momentum of the candidate. This ratio is required to be less than 0.3 (0.6) for the tracker-only (tracker-plus-muon) selection.

Clean separation between HSCPs and SM particles can be achieved by selecting candidates with large p_{T}, large dE/dx, and large TOF (when applicable). These quantities are expected to be uncorrelated for MIPs, while a slow-moving HSCP would have large dE/dx and large TOF even at high p_{T}. Figure 3 shows strong discriminating power for the HSCP signal using I_{as}, TOF, and p_{T}.

5 Background Determination and Search Optimization

As in [5], the mass measurement is based on the relationship:

$$I_h = K\frac{m^2}{p^2} + C. \tag{6}$$

with $K = 2.559 \pm 0.001$ MeV cm^{-1} c^2 and $C = 2.772 \pm 0.001$ MeV cm^{-1}. The search is performed as a counting experiment in a mass window that depends on the tested HSCP mass, M. The mass window extends from $M_{reco} - 2 \times \sigma$ to 2000 GeV/c^2 where σ is the mass resolution expected at the mass M and M_{reco} is the average reconstructed mass for an HSCP of mass M. The values of M_{reco} and σ are obtained from MC simulations.

The candidates passing the pre-selection described in Sec. 4 are used for the signal search and background estimate. For the tracker-only selection, signal candidates are required to have I_{as} and p_{T} greater than the threshold values. A method that exploits the absence of correlation between the p_{T} and dE/dx measurements in data is used to estimate the background from MIPs. The number of candidates that are expected to pass both the final p_{T} and I_{as} thresholds is estimated as $D = BC/A$, where A is the number of candidates that fail both the I_{as} and p_{T} selections and B (C) is the number of candidates that pass only the I_{as} (p_{T}) selection. The B and C candidates are then used to form a binned probability density function in I_h (p) for the D candidates. Finally, using the mass determination (Eq. 6), the full mass spectrum of the background in the signal region D is predicted. However, it is observed that the η distribution of the candidates at low dE/dx is significantly different than that of the candidates at high dE/dx. The η dependence of dE/dx can bias the background prediction when the latter is given in a mass range because the p distribution is η dependent. In order to correct for this effect, events in the C region are weighted so that their η distribution is the same as that in region B.

For the tracker-plus-muon selection, the method is extended by including the TOF measurement and assuming lack of correlation between the TOF, p_T, and dE/dx measurements. With three independent and non-correlated variables, the estimation of the number of background candidates in the signal region can be obtained with six different and independent combinations of three out of the eight exclusive samples, each characterized by candidates passing or not the three thresholds. These eight samples are equivalent to the A, B, C, and D samples in the case of only two measurements. An additional independent background estimation in the signal region D can be obtained with a combination of four out of the eight samples. The corresponding expression is $D = AGF/E^2$, where E is the number of candidates that fail all

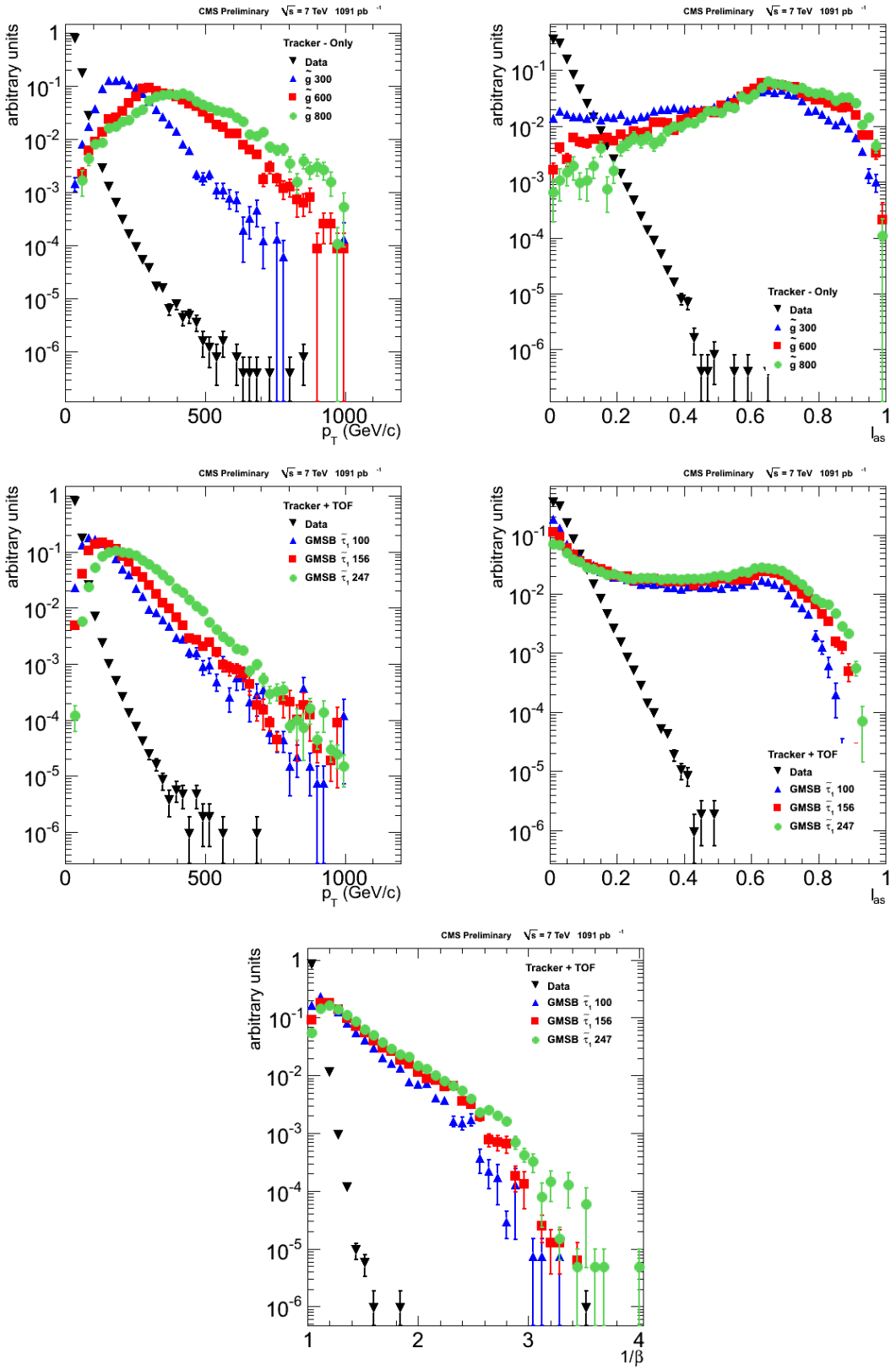

Figure 3: Distributions in data and simulated signal for p_{T}, $1/\beta$, and I_{as}. The upper two figures are for the tracker only selection. The lower three figures are for the tracker plus muon selection. Note that different signal samples are used for the upper and lower figures.

Table 1: Selections used to create the large statistics "loose" sample and results of their application.

Loose	p_T^{cut}	I_{as}^{cut}	TOF^{cut}	Exp.	Obs.
Tk+TOF	40	0.05	1.05	12622 $\pm$ 69 (stat) $\pm$ 1262 (syst)	10562
Tk-Only	40	0.10	/	82530 $\pm$ 199 (stat) $\pm$ 8253 (syst)	74950

selections and A, G and F are the number of candidates that pass only the I_{as}, p_{T} and TOF selection, respectively. This latter estimation is actually the one that suffers from the smallest statistical uncertainties as the four samples are such that at most one of the three thresholds is passed in each of them. For this reason the background estimation is taken from this combination. In order to correct for η differences events in the G region are weighted so that their η distribution is the same as that in region B. The systematic uncertainty on the expected background in the signal region is estimated to be 10% from the scatter of the different independent background estimations. The same uncertainty is also adopted for the tracker-only selection. The statistical uncertainty of the background estimation in either the signal region or in any given mass range is obtained by generating pseudo-experiments drawn from the observed distributions in the control regions.

A "loose" data sample is created such that there is a relatively large number of background candidates and therefore allows us to compare the background prediction with the observed data. Table 1 enumerates the results of this search for the loose selection. Figure 4 shows good agreement between the observed and predicted mass spectrum obtained using the loose selection for the tracker-plus-muon and tracker-only candidates.

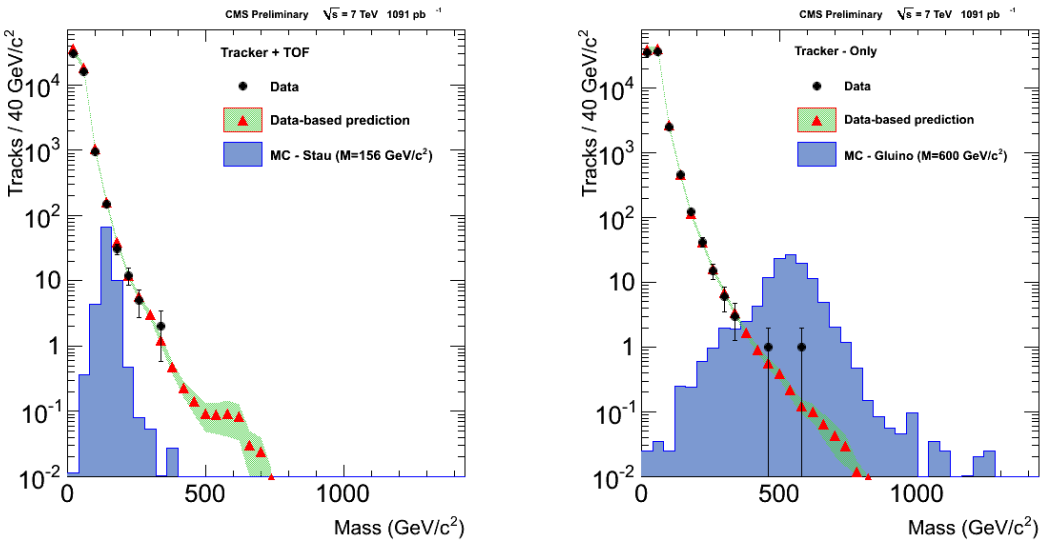

Figure 4: Distribution of the candidate mass for the loose selection defined in Table 1 for the tracker-plus-muon (left) and tracker-only (right) candidates. Shown are: observed spectrum (black dots with the error bars), data-based predicted background spectrum (red triangles) with its uncertainty (green band), and signal simulation (blue shaded histogram).

The final selection criteria for p_{T}, I_{as}, and TOF are optimized for each signal mass by minimizing the expected 95% C.L. cross-section upper limit.

6 Systematic Uncertainties

The main sources of systematic uncertainties on the cross section upper limit and mass lower limit results are broken down into signal acceptance, background estimation, and all other uncertainties.

Simulation is used to determine the signal acceptance. A number of studies have been carried out to estimate how well the simulation models HSCPs and to therefore assess an uncertainty on the acceptance.

The uncertainty on the trigger efficiency measured in the MC is evaluated separately for the E_t^{miss} and single muon triggers. The uncertainty on the E_t^{miss} trigger efficiency is expected to be dominated by the uncertainty of $3-6\%$ on the jet energy scale [24]. Increasing the threshold on the E_t^{miss} trigger by 6% resulted in a change in the corresponding trigger efficiency by $\sim 1\%$ for all considered signals. For the single muon trigger, a disagreement of up to 10% is observed between the single muon trigger efficiency in data and MC at all energies [23]. In addition, for this specific analysis, it is expected that a further uncertainty arises from imperfect simulation of the synchronization of the muon trigger electronics. The latter effect is found to yield less than 5% uncertainty on the overall signal acceptance. Assuming a drop in the muon trigger efficiency by 15%, it was verified that the drop in the overall trigger efficiency is less than 5% for all considered signals. On the basis of these numbers, an uncertainty of 5% on the overall trigger efficiency was assumed.

The uncertainty on the track momentum scale is estimated by varying track p_{T} by

$$\frac{1}{p'_{\mathrm{T}}} = \frac{1}{p_{\mathrm{T}}} + \delta_{K_T}(q,\phi,\eta) \tag{7}$$

$$\delta_{K_T}(q,\phi,\eta) = A + B\eta^2 + qC\sin(\phi-\phi_0) \tag{8}$$

where A = 0.236 TeV^{-1}, B = -0.135 TeV^{-1}, C = 0.282 TeV^{-1}, and ϕ_0 = 1.337. The difference between the signal acceptance with the nominal and shifted p_{T} is taken as the uncertainty. It is found to be $<$5%.

The uncertainty on the dE/dx simulation is estimated by varying the I_{as} discriminator by 3%. This results in a change in the signal acceptance by up to 13% for the lowest mass points, and a few percent for the rest in the tracker-only selection. The changes are a few percent less in the tracker-plus-muon selection. A shift in dE/dx would have only minimal effect on I_h since it would also result in a shift in the parameters of Eq. 3 in [25]. The I_h value will not change significantly and the uncertainty on I_h is found to be $< 1\%$.

The uncertainty on offline track ($< 2\%$ [26]) and muon (5% [23]) reconstruction efficiency are also included.

Finally, two theoretical uncertainties are difficult to evaluate, the uncertainty on the model of hadronization and nuclear interaction, and the uncertainty due to the MPI tune. The hadronization and nuclear interaction model is discussed in Sec. 2 with results evaluated for two different hadronization schemes for the gluino result. As discussed in Sec. 2, the analysis is done with tune D6T. Tune Z2 uses a p_{T}-ordered model which appears to generate significantly more initial state radiation (ISR) than the Q^2-ordered D6T model. The trigger efficiency and the reconstruction efficiency increase dramatically such that our observed limits get much better (for example, in the gluino mass range 600–800 GeV, the cross section limit improves by 40% for the Tune Z2 samples). To be conservative, we only use the Q^2-ordered D6T for the reported limits.

Table 2: Sources of systematic errors and corresponding relative uncertainties.

Source of Systematic Error	Relative Uncertainty (%)
Signal efficiency	
Trigger efficiency	5
Muon reconstruction efficiency	5
Track reconstruction efficiency	< 2
Track momentum scale	< 5
Ionization energy loss scale (I_{as})	$[5, 10]$
Ionization energy loss scale (I_h)	< 1
Total uncertainty on signal acceptance	$[10, 15]$
Expected background	10
Integrated luminosity	6

In addition, there is an uncertainty on the theoretical cross section for production of top squarks and gluino pairs. These uncertainties were provided by the authors of [27–31] and vary in the range 10% to 25%, being larger for the heavier masses. The main sources of uncertainty are the renormalization and factorization scales and the parton distribution functions. The uncertainty on the theoretical cross section for production of staus in the considered models has not been estimated at this stage. The theoretical cross section uncertainty is not included in the final result.

The following additional uncertainties are incorporated in the analysis:

- Uncertainty on the absolute value of the integrated luminosity. An uncertainty of 6% is assumed.
- Uncertainty on the expected background. This contribution was discussed in Section 5 and is estimated to be of the order of 10%. Due to the small numbers of expected events for most mass points, this uncertainty does not radically change results.

These uncertainties are summarized in Table 2 and are incorporated in the quoted limits.

7 Results

By comparing data in the signal region with the expected background, we can set upper limits on HSCP production at the 95% C.L. for each of the optimized model and mass points. The acceptance for the signal for the various combinations of selection and scenario is determined from MC. There is no evidence of significant excess of data compared to the expected background over the mass range of interest.

The cross section upper limits at 95% C.L. are computed with a full Bayesian method that uses a lognormal prior [32, 33] for integration over the nuisance parameters and a flat prior for the parameter of interest. The tracker-only selection provides better limits than the tracker-plus-muon selection for all scenarios for stop and gluino, in particular for the pessimistic one of charge suppression. The cross section upper limit curves obtained with both selections are reported in Fig. 5, along with the theoretical predictions for $\tilde{t}_1$ and $\tilde{g}$ pair production computed at NLO+NLL [27–30] using PROSPINO [34]. As discussed in Sec. 6, a relative uncertainty in the range 10% to 25% is included in the figure as a band around the central value. The systematic uncertainties discussed in section 6 are included in the reported cross-section upper limits.

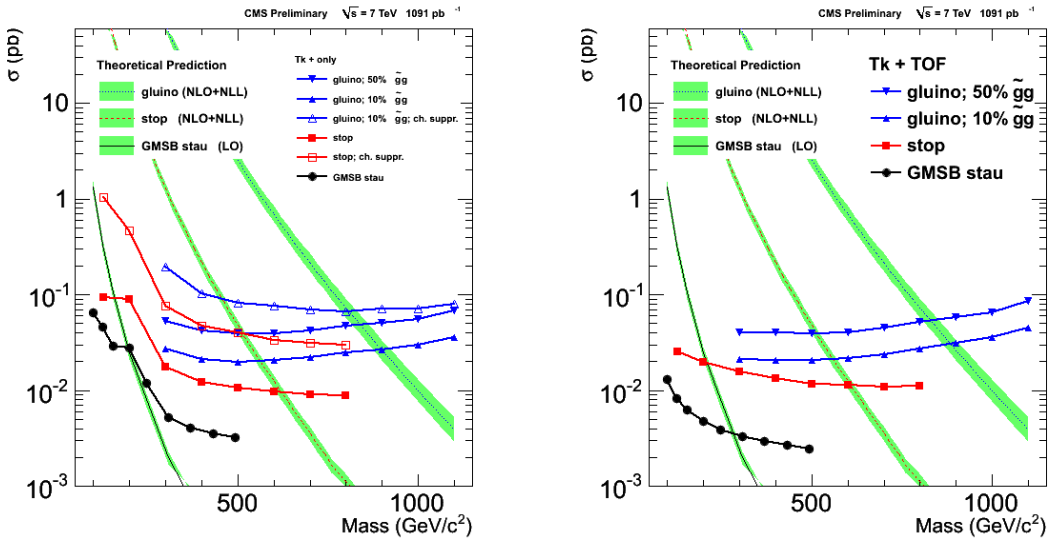

Figure 5: Predicted theoretical cross section and observed 95% C.L. upper limits on the cross section for the different combinations of models and scenarios considered: pair production of supersymmetric stop and gluinos; different fractions, f, of R-gluonball states produced after hadronization and charge suppression (ch. suppr.) scenarios. Left: tracker-only selection. Right: tracker-plus-muon. The bands represent the theoretical uncertainties on the cross section values.

From the intersection of the cross section limit curve and the center of the theoretical cross section band, a 95% C.L. lower limit of 899 (839) GeV/c^2 on the mass of pair-produced $\tilde{g}$, hadronizing into stable R-gluonballs with 10% (50%) probability, is set with the tracker-only selection. The tracker-plus-muon selection gives a lower limit of 885 (829) GeV/c^2 for the same signal model. The analogous limit on the $\tilde{t}_1$ mass is 620 GeV/c^2 with the tracker-only selection and 608 GeV/c^2 with the tracker-plus-muon selection. The charge suppression scenario discussed above yields a $\tilde{g}$ mass limit of 808 GeV/c^2 for $f = 10\%$ and 515 GeV/c^2 for the $\tilde{t}_1$. The limits on staus are set at $>$293 GeV/c^2 with the tracker-plus-muon selection.

8 Conclusions

In summary, the CMS detector has been used to identify highly ionizing, high-p_T particles and measure their masses. Two searches have been conducted: a very inclusive and model independent one that uses highly-ionizing tracks reconstructed in the inner tracker detector, and another requiring also that these tracks be identified in the CMS muon system and have long TOF. In each case, the observed distribution of the candidate masses is consistent with the expected background. We have set lower limits on masses of stable weakly and strongly interacting supersymmetric particles.

References

[1] M. Fairbairn et al., "Stable massive particles at colliders", *Phys. Rept.* **438** (2007) 1, arXiv:hep-ph/0611040. doi:10.1016/j.physrep.2006.10.002.

[2] C. W. Bauer, Z. Ligeti, M. Schmaltz et al., "Supermodels for early LHC", *Phys. Lett.* **B690** (2010) 280–288, arXiv:0909.5213. doi:10.1016/j.physletb.2010.05.032.

[3] ATLAS Collaboration Collaboration, "Search for Heavy Long-Lived Charged Particles with the ATLAS detector in pp collisions at sqrt(s) = 7 TeV", arXiv:1106.4495. * Temporary entry *.

[4] ATLAS Collaboration, "Search for stable hadronising squarks and gluinos with the ATLAS experiment at the LHC", arXiv:1103.1984.

[5] CMS Collaboration, "Search for Heavy Stable Charged Particles in pp collisions at sqrt(s)=7 TeV", *JHEP* **03** (2011) 024, arXiv:1101.1645. doi:10.1007/JHEP03(2011)024.

[6] CDF Collaboration, "Search for Long-Lived Massive Charged Particles in 1.96 TeV $\bar{p}p$ Collisions", *Phys. Rev. Lett.* **103** (2009) 021802, arXiv:0902.1266. doi:10.1103/PhysRevLett.103.021802.

[7] D0 Collaboration, "Search for Long-Lived Charged Massive Particles with the D0 Detector", *Phys. Rev. Lett.* **102** (2009) 161802, arXiv:0809.4472. doi:10.1103/PhysRevLett.102.161802.

[8] M. Drees and X. Tata, "Signals for heavy exotics at hadron colliders and supercolliders", *Phys. Lett.* **B252** (1990) 695. doi:10.1016/0370-2693(90)90508-4.

[9] G. F. Farrar, R. Mackeprang, D. Milstead et al., "Limit on the mass of a long-lived or stable gluino", *JHEP* **02** (2011) 018, arXiv:1011.2964. doi:10.1007/JHEP02(2011)018.

[10] G. R. Farrar and P. Fayet, "Phenomenology of the Production, Decay, and Detection of New Hadronic States Associated with Supersymmetry", *Phys. Lett.* **B76** (1978) 575.

[11] R. Mackeprang and D. Milstead, "An Updated Description of Heavy-Hadron Interactions", *Eur. Phys. J.* **C66** (2010) 493, arXiv:0908.1868. doi:10.1140/epjc/s10052-010-1262-1.

[12] D0 Collaboration, "Search for stopped gluinos from $p\bar{p}$ collisions at $\sqrt{s}$ = 1.96 TeV", *Phys. Rev. Lett.* **99** (2007) 131801, arXiv:0705.0306. doi:10.1103/PhysRevLett.99.131801.

[13] CMS Collaboration, "Search for Stopped Gluinos in pp Collisions at $\sqrt{s} = 7$ *TeV*", *Phys. Rev. Lett.* **106** (2011) 011801, arXiv:1011.5861. doi:10.1103/PhysRevLett.106.011801.

[14] CMS Collaboration, "The CMS experiment at the CERN LHC", *JINST* **0803** (2008) S08004. doi:10.1088/1748-0221/3/08/S08004.

[15] T. Sjöstrand, S. Mrenna, and P. Z. Skands, "PYTHIA 6.4 Physics and Manual", *JHEP* **05** (2006) 026, arXiv:hep-ph/0603175. doi:10.1088/1126-6708/2006/05/026.

[16] A. C. Kraan, "Interactions of heavy stable hadronizing particles", *Eur. Phys. J.* **C37** (2004) 91, arXiv:hep-ex/0404001. doi:10.1140/epjc/s2004-01997-7.

[17] R. Mackeprang and A. Rizzi, "Interactions of coloured heavy stable particles in matter", *Eur. Phys. J.* **C50** (2007) 353, arXiv:hep-ph/0612161. doi:10.1140/epjc/s10052-007-0252-4.

[18] G. F. Giudice and R. Rattazzi *Phys. Rept.* **322** (1999) 419–499, arXiv:hep-ph/9801271.

[19] B. C. Allanach et al. *Eur. Phys. J.* **C25** (2002) 113–123, arXiv:hep-ph/0202233.

[20] F. E. Paige, S. D. Protopopescu, H. Baer et al. arXiv:hep-ph/0312045.

[21] CMS Collaboration, "Jet performance in pp collisions at $\sqrt{s}$=7TeV", *CMS Physics Analysis Summary* **CMS-PAS-JME-10-003** (2010).

[22] M. Cacciari, G. P. Salam, and G. Soyez, "The anti-k_t jet clustering algorithm", *JHEP* **04** (2008) 063, arXiv:0802.1189. doi:10.1088/1126-6708/2008/04/063.

[23] CMS Collaboration, "Performance of muon identification in pp collisions at $\sqrt{s}$ = 7 TeV", *CMS Physics Analysis Summary* **CMS-PAS-MUO-10-002** (2010).

[24] CMS Collaboration, "Jet Energy Corrections determination at 7 TeV", *CMS Physics Analysis Summary* **CMS-PAS-JME-10-010** (2010).

[25] CMS Collaboration, "Search for Heavy Stable Charged Particles in pp Collisions at $\sqrt{s}$=7TeV", *CMS Physics Analysis Summary* **CMS-PAS-EXO-10-011** (2010).

[26] CMS Collaboration, "Measurement of Tracking Efficiency", *CMS Physics Analysis Summary* **CMS-PAS-TRK-10-002** (2010).

[27] A. Kulesza and L. Motyka, "Threshold resummation for squark-antisquark and gluino-pair production at the LHC", *Phys. Rev. Lett.* **102** (2009) 111802, arXiv:0807.2405. doi:10.1103/PhysRevLett.102.111802.

[28] A. Kulesza and L. Motyka, "Soft gluon resummation for the production of gluino-gluino and squark-antisquark pairs at the LHC", *Phys. Rev.* **D80** (2009) 095004, arXiv:0905.4749. doi:10.1103/PhysRevD.80.095004.

[29] W. Beenakker et al., "Soft-gluon resummation for squark and gluino hadroproduction", *JHEP* **12** (2009) 041, arXiv:0909.4418. doi:10.1088/1126-6708/2009/12/041.

[30] W. Beenakker et al., "Supersymmetric top and bottom squark production at hadron colliders", *JHEP* **08** (2010) 098, arXiv:1006.4771. doi:10.1007/JHEP08(2010)098.

[31] W. Beenakker et al., "Squark and gluino hadroproduction", *Int. J. Mod. Phys.* **A26** (2011) 2637–2664, arXiv:1105.1110. doi:10.1142/S0217751X11053560.

[32] W. T. Eadie, D. Drijard, F. E. James et al., "Statistical Methods in Experimental Physics". North Holland, Amsterdam, 1971.

[33] F. James, "Statistical Methods in Experimental Physics". World Scientific, Singapore, 2006.

[34] W. Beenakker, R. Hopker, and M. Spira, "PROSPINO: A program for the PROduction of Supersymmetric Particles In Next-to-leading Order QCD", arXiv:hep-ph/9611232.